

---

# Gene network robustness as a multivariate character

Arnaud Le Rouzic<sup>1,\*</sup>

**1 Laboratoire Évolution: Génomes, Comportement, Écologie;**  
**Université Paris-Saclay, CNRS, IRD.**

\* [arnaud.le-rouzic@egce.cnrs-gif.fr](mailto:arnaud.le-rouzic@egce.cnrs-gif.fr)

## Abstract

Robustness to genetic or environmental disturbances is often considered as a key property of living systems. Yet, in spite of being discussed since the 1950s, how robustness emerges from the complexity of genetic architectures and how it evolves still remains unclear. In particular, whether or not robustness to various sources of perturbations is independent conditions the range of adaptive scenarios that can be considered. For instance, selection for robustness to heritable mutations is likely to be modest and indirect, and its evolution might result from indirect selection on a pleiotropically-related character (e.g., homeostasis) rather than adaptation. Here, I propose to treat various robustness measurements as quantitative characters, and study theoretically, by individual-based simulations, their propensity to evolve independently. Based on a simple evolutionary model of a gene regulatory network, I showed that different ways to measure the robustness of gene expression to genetic or non-genetic disturbances were substantially correlated. Yet, robustness was evolvable in several dimensions, and robustness components could evolve differentially under direct selection pressure. Therefore, the fact that the sensitivity of gene expression to e.g. mutations and environmental factors rely on the same gene networks does not preclude that robustness components may have distinct evolutionary histories.

## 1 Introduction

Robustness is the capacity of living organisms to buffer internal or environmental disturbances. Robustness encompasses, for instance, the ability to maintain physiological equilibria (homeostasis), to ensure developmental stability, or to repair and mitigate DNA damage in both soma and germline. Although robustness is virtually intermingled with the definition of life itself, its underlying mechanisms and its evolutionary origins remain far from being clearly understood (Stearns, 2002; Masel and Siegal, 2009; Wagner, 2013; Hallgrímsson et al., 2019).

Robustness can evolve as a consequence of non-linearities in the developmental process, i.e. changes in the magnitude of the effect of some genetic or environmental factor on the phenotype of interest (Nijhout, 2002). The study of the evolutionary mechanisms leading to robustness roots into the conceptual and empirical work by C.H. Waddington and the concept of canalization (Waddington, 1942; Schmalhausen, 1949; Waddington, 1959; Loison, 2019). Canalization is a property of complex developmental systems that buffers environmental and genetic variation, and maintains actively the organism in an optimal developmental path. Although

---

the scope and the definition of canalization varies substantially among authors, canalization is generally expected to evolve as an adaptation to "canalizing" selection for an optimal phenotype (Eshel and Matessi, 1998; Debat and David, 2001; Flatt, 2005; Klingenberg, 2019). However, formal population genetic models have questioned the unicity of the canalization process. In particular, robustness to environmental factors appears more likely to evolve as an adaptation than robustness to genetic (mutational) disturbances, on which selection seems to be rather weak and indirect even in optimal theoretical conditions (Wagner et al., 1997; Hermisson et al., 2003; Le Rouzic et al., 2013).

In this context, the evolution of robustness as a general property of the organisms heavily depends on the genetic and physiological integration of the different robustness dimensions (Fares, 2015). If the robustness to environmental factors and to genetic mutations share the same physiological bases, the adaptive evolution of environmental canalization could generate a correlated response of genetic canalization; this hypotheses has been referred to as "congruent evolution" (Visser et al., 2003). In contrast, if genetic and environmental robustness were independent biological mechanisms, they would be featured by independent evolutionary mechanisms, and possibly independent evolutionary histories.

Although this issue would benefit from a better theoretical framework, modelling the evolution of robustness is not straightforward. The simplest approach relies on focusing on modifiers, i.e. genes that can influence the robustness of the organism without affecting the phenotype. However, in the case of genetic robustness, modifier-based models either rely on tricky rescaling or do not dissociate the phenotype and the robustness to the phenotype (Wagner et al., 1997; Kawecki, 2000; Rajon and Masel, 2013). In addition, in models where the genotype-phenotype association is arbitrary, any correlation between e.g. environmental and genetic robustness is a modelling choice, and not an output of the model. More promising to address the congruent evolution issue are models in which the phenotype is a result of an integrated process mimicking some developmental or physiological mechanism. In such dynamic models, robustness to various disturbances appear as an emergent property of the model complexity, caused by regulatory feedbacks, that cannot be easily deduced from the model parameters. Although the potential palette of relevant dynamic models is large and could include e.g. morphological development models (Milocco and Salazar-Ciudad, 2020) or metabolic models (Nijhout et al., 2019), evolutionary biologists have often considered gene regulatory network models as a good compromise between complexity and numerical tractability for studying the evolution of canalization and robustness (Kauffman, 1969; Wagner, 1994; Smolen et al., 2000; Le Cunff and Pakdaman, 2012).

Such theoretical gene networks have been shown to display enough non-linearities (epistasis and pleiotropy) to evolve enhanced or reduced sensitivity to environmental (Masel, 2004; Espinosa-Soto et al., 2011; Espinoza-Soto et al., 2011) and genetic (Wagner, 1996; Bergman and Siegal, 2003; Draghi and Wagner, 2009; Azevedo et al., 2006; Rünneburger and Le Rouzic, 2016) perturbations. Interesting observations suggest that environmental or genetic canalization could be correlated to other robustness properties in such models. In particular, it has been shown that network stability, the propensity of the network to maintain stable (non-cyclic) gene expressions, was positively correlated to robustness, as selection on stability alone could drive an indirect response of genetic (Siegal and Bergman, 2002) and environmental (Masel, 2004) canalization. In contrast, Odorico et al. (2018) showed that networks selected to maintain (but not converge to) an equilibrium could become both environmentally sensitive and genetically canalized, suggesting that environmental and genetic robustness could be theoretically

decoupled. However, no systematic quantitative description of the pleiotropic pattern underlying different robustness components has never been attempted.

Here, I aim at extending the study of canalization in theoretical gene networks to address the multidimensional nature of robustness, by estimating the evolutionary independence of various robustness components. Five robustness-related measurements were considered, two of them corresponding to environmental robustness (early vs. late disturbances), two corresponding to genetic robustness (early — inherited — or late — acquired — mutations), the last one (gene expression instability) being related to the intrinsic stability of the expression phenotype. The first part of this study focuses on the multidimensional patterns of robustness in small and random networks, and the second part on the evolutionary consequences of the pleiotropic nature of robustness, through individual-based simulations.

## 2 Model and Methods

### 2.1 Gene regulatory network

The network model is derived from Wagner (1994) and Wagner (1996) and belongs to the family of gene regulatory network models sometimes referred to as "Wagner model" (see Fierst and Phillips, 2015 for a historical record). The main difference with Wagner (1996) and further work is that the network output (gene expressions) is quantitative and not qualitative, in the same way as in Siegal and Bergman (2002).

More specifically, the structure of a  $n$ -gene network is encoded as a  $n \times n$  matrix  $\mathbf{W}$ , while the state of the network is stored into a vector of size  $n$ ,  $\mathbf{P}$ . In this setting,  $W_{ij}$  encodes the influence of gene  $j$  on the expression of gene  $i$ ,  $W_{ij} < 0$  represents a negative interaction (inhibition),  $W_{ij} > 0$  a positive interaction (activation), and  $W_{ij} = 0$  denotes the absence of regulatory interaction.  $P_i$  is the expression of gene  $i$ , ranging between 0 (no expression) and 1 (maximum expression).

The properties of these gene networks are explored in a discrete dynamic system:

$$\mathbf{P}_{t+1} = F(\mathbf{WP}_t), \quad (1)$$

where the function  $F$  is a vectorized version of a sigmoid scaling function:  $F(x_1, x_2, \dots, x_n) = [f(x_1), f(x_2), \dots, f(x_n)]$ ;

$$f(x) = \frac{1}{1 + \lambda_a e^{-\mu_a x}}, \quad (2)$$

with  $\lambda_a = (1 - a)/a$  and  $\mu_a = 1/a(1 - a)$ . The function  $f$  is scaled such that  $f(0) = a$  and  $df/dx|_{x=0} = 1$ ; the parameter  $a$  thus stands for the constitutive gene expression (the expression of a gene in absence of regulators), and this function defines the scale of the matrix  $\mathbf{W}$ :  $W_{ij} = \delta$  ( $\delta \ll 1$ ) means that the expression of gene  $i$  at the next time step will tend to  $P_{i,t+1} = a + \delta$  if  $i$  is regulated by a single, fully expressed gene  $j$  ( $P_{j,t} = 1$ ).

Gene networks dynamics started from an initial expression  $\mathbf{P}_0$ , and gene expression was updated for  $T$  timesteps. By default,  $\mathbf{P}_0 = (a, a, \dots, a)$ , since this step immediately follows a virtual initial state with no expression. The expression phenotype corresponding to a gene network was determined by averaging gene expressions during the last  $\tau$  timesteps for each gene  $i$ :  $P_i^* = (1/\tau) \sum_{t=T-\tau}^T P_{it}$ .

---

## 2.2 Robustness indicators

Five robustness indicators were calculated, corresponding to five different aspects of genetic or environmental robustness in a gene network: network stability  $\rho_S$ , robustness to early ( $\rho_E$ ) and late ( $\rho_e$ ) environmental disturbance, and robustness to early ( $\rho_M$ ) and late ( $\rho_m$ ) genetic disturbance. All indicators were expressed on a scale homogeneous to log variances in gene expressions; the mode of calculation is summarized in Table 1.

Dynamic systems based on the Wagner model often tend to generate limit cycles and never converge to a stable equilibrium. Network stability  $\rho_S$  quantifies the capacity for a specific network to lead to stable gene expressions. For consistency with other indicators, this instability was measured as the log squared difference between the average expression during the last  $\tau$  timesteps, and an extra timestep.

The robustness to early environmental disturbance  $\rho_E$  measures the capacity of a network to reach a consistent final state starting from different initial gene expressions. In practice,  $R$  replicates of the network dynamics were run, in which the initial gene expressions ( $\mathbf{P}_0$ ) were drawn into Gaussian ( $\mu = a, \sigma = \sigma_E$ ) distributions (expression values  $< 0$  and  $> 1$  were fixed to 0 and 1, respectively). The environmental robustness for each gene  $i$  was measured as the log variance in the final gene expression across these replicates.

The robustness to late environmental disturbance  $\rho_e$  measures the capacity of a network to recover its equilibrium state after having been disturbed. Gene expressions after  $T$  timesteps were disturbed by adding a random Gaussian noise of standard deviation  $\sigma_e$  to each gene of the network, and  $\rho_{ei}$  was computed for each gene  $i$  as the log variance in gene expression at time step  $T + 1$  over  $R$  replicates.

The robustness to early mutations  $\rho_M$  measures the system robustness to inherited genetic mutations (modifications of the  $\mathbf{W}$  matrix). A random non-zero element of the  $\mathbf{W}$  matrix was shifted by a random Gaussian number of standard deviation  $\sigma_M$ , and its consequences on the mean expression of all network genes was recorded. The procedure was replicated  $R$  times, and the robustness score  $\rho_{Mi}$  for each gene  $i$  was calculated as the log variance of gene expression across  $R$  replicates.

Finally, the robustness to late mutations  $\rho_m$  measured the effect of mutations in the gene network  $\mathbf{W}$  after having reached the final state. In practice, the  $\mathbf{W}$  matrix was mutated in the same way as for  $\rho_M$  with a standard deviation  $\sigma_m$ , but its consequences on gene expression were calculated for only one timestep, starting from the last state of the network. The robustness score was calculated as for other indicators (log variance over  $R$  replicates).

All these scores were calculated for every gene  $i$  of a given network, and then averaged over all genes in order to get a series of summary network descriptors. The magnitude of the score itself is arbitrary, as it depends on the size of the disturbance. However, indicators happen to increase approximately linearly with the size of the disturbance (Appendix 1), suggesting the the results would be largely unaffected by a change in the variance of mutational effects and environmental noise.

---

## 2.3 Random networks

Random networks were generated as  $n \times n$  matrices filled with independent identically-distributed random numbers drawn into a Gaussian ( $\mu_0 = 0, \sigma_0 = 1$ ) distribution. A density parameter  $1/n \leq d \leq 1$  could be specified, corresponding to the frequency of non-zero slots in the  $\mathbf{W}$  matrix. Zeros were placed randomly, with the constraint that all genes should be regulated by at least another one.

Indicator	Robustness component	Computation	Disturbance std. dev.
$\rho_S$	Expression stability	$\rho_{S,i} = \log(P_i^* - \bar{P}_{T+1})^2$	
$\rho_E$	Early noise in gene expression	$\rho_{E,i} = \log[\frac{1}{R-1} \sum_{r=1}^R (P_{i,r}^* - \bar{P}_i^*)^2]$	$\sigma_E = 0.1$
$\rho_e$	Late noise in gene expression	$\rho_{e,i} = \log[\frac{1}{R-1} \sum_{r=1}^R (P_{i,T+1,r} - \bar{P}_{i,T+1})^2]$	$\sigma_e = 0.1$
$\rho_M$	Early (inherited) mutations	$\rho_{M,i} = \log[\frac{1}{R-1} \sum_{r=1}^R (P_{i,r}^* - \bar{P}_i^*)^2]$	$\sigma_M = 0.1$
$\rho_m$	Late (acquired) mutations	$\rho_{m,i} = \log[\frac{1}{R-1} \sum_{r=1}^R (P_{i,T+1,r} - \bar{P}_{i,T+1})^2]$	$\sigma_m = 0.1$

Table 1: Summarized calculation of all five robustness indicators. Index  $i$  stands for the gene ( $1 \leq i \leq n$ ), and  $r$  for the replicate ( $1 \leq r \leq R$ ), since all indicators except  $\rho_S$  were estimated by a resampling procedure.  $P_i^*$  stand for the average gene expression of the network (mean expression from the last  $\tau$  timesteps), and  $\bar{P}_i = (1/R) \sum_{r=1}^R P_{i,r}^*$  represents the mean over replicates. Noise in gene expression was simulated by adding a random Gaussian deviation to the initial state of the network (for  $\rho_E$ ) or to the last state of the network (for  $\rho_e$ ). Mutations were simulated by adding a random deviation to a random interaction in the network, either before starting the network dynamics ( $\rho_M$ ) or after the last time step ( $\rho_m$ ). All robustness indicators are homogeneous to a log variance in gene expression; robustness increases when the indicator gets smaller, and sensitivity increases when the indicator increases. The last column indicates the standard deviation of the corresponding Gaussian disturbance.

## 2.4 Exhaustive exploration of two-gene networks

The main interest of gene-network models is the complexity and the richness of the underlying genotype-phenotype relationship. As a side effect, such models are in general difficult to handle mathematically (Carneiro et al., 2011; Le Cunff and Pakdaman, 2012). Excluding the one-gene self-regulating case (which already has non-trivial mathematical properties, Guyeux et al., 2018), the simplest network (2-by-2 matrix) has four genetic parameters, which makes the exploration of the parameter set tedious. Here, the number of dimensions was restricted by considering the set of networks that lead to a predefined arbitrary equilibrium,  $\mathbf{P}_\infty^\theta = (P_1^\theta, P_2^\theta)$ . As  $F(\mathbf{W}\mathbf{P}_\infty^\theta) = \mathbf{P}_\infty^\theta$ , the  $\mathbf{W}$  matrix can be reduced to two independent parameters,  $W_{11}$  and  $W_{21}$ :

$$\mathbf{W} = F \begin{bmatrix} (W_{11} & A) & \begin{pmatrix} P_1^\theta \\ P_2^\theta \end{pmatrix} \end{bmatrix} = \begin{pmatrix} P_1^\theta \\ P_2^\theta \end{pmatrix}, \quad (3)$$

with

$$\begin{aligned} A &= \frac{1}{P_2^\theta} [f^{-1}(P_1^\theta) - W_{11}P_1^\theta], \\ B &= \frac{1}{P_2^\theta} [f^{-1}(P_2^\theta) - W_{21}P_1^\theta], \end{aligned} \quad (4)$$

$f^{-1}(x) = -\frac{1}{\mu_a} \log\left(\frac{1-x}{\lambda_a x}\right)$  being the inverse of  $f(x)$  (equation 2). The  $\mathbf{W}$  matrix achieving the desired  $\mathbf{P}_\infty^\theta$  equilibrium from a specific pair  $W_{11}, W_{21}$  always exists (and is unique), but the stability of the equilibrium is not guaranteed. Networks which final gene expression  $\mathbf{P}^* = (P_1^*, P_2^*)$  differed substantially from the target (in practice, when  $|P_1^* - P_1^\theta| + |P_2^* - P_2^\theta| > 0.15$ ) were excluded from the analysis. Such discrepancies correspond to either unstable equilibria (in which case gene expressions were driven away from the equilibrium) or extreme oscillatory behaviors

---

(large oscillations may hit extreme expression limits (0 or 1), which drives the average expression away from the target equilibrium).

## 2.5 Evolutionary simulations

The evolution of gene networks under various evolutionary constraints was studied by individual-based simulations. Each individual was featured by its genotype (a  $n \times n$   $\mathbf{W}$  matrix, by default  $n = 6$ ), its expression phenotype  $\mathbf{P}^*$ , and the five robustness scores  $\rho_S$ ,  $\rho_E$ ,  $\rho_e$ ,  $\rho_M$ , and  $\rho_m$ . Individuals were haploid and reproduced clonally. Mutations consisted in adding a random Gaussian deviate of variance  $\sigma_\nu^2$  to an element of the  $\mathbf{W}$  matrix, with a rate  $\nu$  per individual and per generation. Generations were non-overlapping, and population size  $N$  was constant. A generation consisted in sampling  $N$  new individuals among the  $N$  parents, with a probability proportional to the individual fitness. Fitness was computed assuming stabilizing selection around a target (optimal) expression level for  $n' \leq n$  genes of the network (by default  $n' = 3$ ), as  $w = \exp(-\sum_{i=1}^{n'} s_i (P_i^* - \theta_i)^2)$ , where  $s_i$  was the strength of stabilizing selection on gene  $i$  ( $s_i = 0$  standing for no selection), and  $\theta_i$  was the optimal expression phenotype. The  $\theta_i$  were drawn in a uniform (0,1) distribution at the beginning of each replicated simulation, and the initial gene network was empty ( $W_{ij} = 0$ ) except for one random element per line, which was initialized to match the optimal expression using equation (4), which can be trivially extended for any number of genes (with only one unknown per line).

In addition, direct, directional selection on robustness indicators was performed in some simulations, consisting in multiplying individual fitness by  $\exp(\sum_{x \in (S, E, e, M, m)} \beta_x \rho_x)$ , where  $\beta_x$  was the strength of directional (positive or negative) selection on robustness index  $x$  (in practice,  $\beta_x = \pm 0.01$ ).

Simulations and data analysis were coded in R (R Core Team, 2020), except for the core gene network dynamics that was coded in C++ and embedded in the R code with the Rcpp package (Eddelbuettel and Balamuta, 2017). Scripts to reproduce simulations and figures are available as a GitHub directory (<https://github.com/lerouzic/robustness>).

## 3 Results

### 3.1 Random networks

Random interaction matrices are regularly used in the literature to study the general properties of gene networks (e.g. Carneiro et al., 2011; Pinho et al., 2012). As such, random networks are not expected to reflect the properties of biologically-realistic genetic architectures, as biological networks are far from random. However, such an approach helps developing a general intuition about the properties of the underlying model, especially about the amount of selection it takes to bring a network into its non-random state.

Correlations were calculated between all five robustness components over 10,000 random networks (Appendix 2). All robustness components were positively correlated. However, correlations ranged from about 0.63 (late genetic vs. early environmental) to above 0.97 (late environmental vs. late genetic). A Principal Component Analysis (Figure 1) confirms that robustness components are not fully correlated. The first PC (82% of the total variance) corresponds to the general robustness of the network, and involves all robustness indexes. The remaining variance is explained by orthogonal vectors separating all other robustness

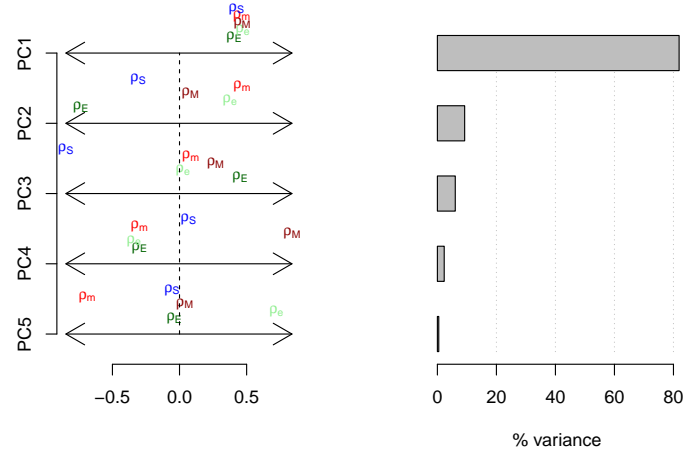


Figure 1: Summary of the principal component analysis on the five robustness components over 10,000 random 6-gene networks ( $\mu_0 = 0, \sigma_0 = 1$ ). Left: position of the five robustness components on all five (normalized) Principal Components (PC);  $\rho_S$ : Stability,  $\rho_E$ : Early environmental,  $\rho_e$ : Late environmental,  $\rho_M$ : Early genetic,  $\rho_m$ : Late genetic. Right: relative contribution of the five PCs to the total variance.

components. At least 4 out of 5 PCs, explaining 10% to 2% of the total variance, did not vanish when increasing the sample size (Appendix 3).

### 3.2 Two-gene networks

In the following, I considered the particular case of  $\mathbf{P}_\infty = (0.3, 0.6)$  with two intermediate, distinct gene expressions. Equivalent results could be achieved with a different target. Figure 2 illustrates how the robustness components varied in this constrained 2-gene network model (red stands for maximum robustness, i.e. minimum scores for  $\rho_S, \rho_E, \rho_e, \rho_M$ , and  $\rho_m$ ). In the white regions, the equilibrium was not achieved in numerical simulations for at least three different reasons (Appendix 4: (i) fluctuations around the equilibrium are large enough to hit the edges of the (0,1) interval, shifting the mean expression; (ii) the expression dynamics was slow and the network was unable to get close to the equilibrium after 16 time steps; (iii) the equilibrium was not reachable from the default starting point.

It immediately appears that the different robustness components were correlated, but do not overlap perfectly. The simulated behavior of networks A to E are illustrated in Appendix 5, and the corresponding  $\mathbf{W}$  matrices are provided in Appendix 6. The network denoted as B was robust to all five components, while network E was sensitive to all components except stability. Network C was unstable, but remained relatively canalized. Networks A and D illustrate intermediate decanalization behaviors, through different mechanisms (unstability for network D, and weak buffering for network A).

This 2-gene network analysis thus confirms the results obtained for larger gene networks. Robustness is thus not a feature of large and intricate genetic architectures, as it is already present (and multidimensional) in the simplest gene networks. The different robustness components are partially independent, even in

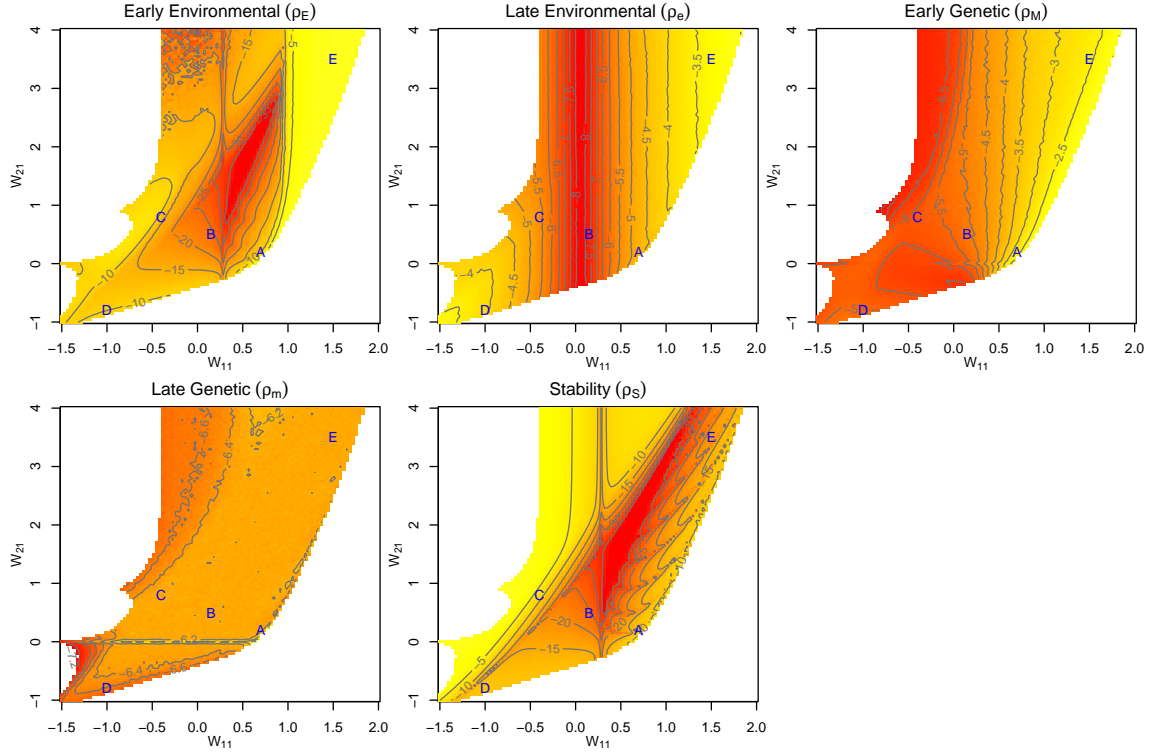


Figure 2: Robustness indicators ( $\rho_S, \rho_E, \rho_e, \rho_M, \rho_m$ ) estimated for an exhaustive continuum of two-gene networks with an arbitrary expression equilibrium at  $\mathbf{P}_\infty = (0.3, 0.6)$ . Although two-gene networks have four independent genetic parameters, only two were represented here, the two others being computed to ensure the desired equilibrium. Red stands for the maximum robustness (lowest variance scores); yellow for minimum robustness (highest scores). For readability, color scales are different across panels. Letters A to E stand for five example networks illustrated in Appendix 5.

small and highly constrained networks. All the networks considered here converge to the same gene expression at time step 20, and can thus be considered as phenotypically equivalent ; the colored space in Figure 2 thus represents a connected neutral network in which populations could evolve, and thus change the topology and the robustness of the gene network, while keeping the expression phenotype constant.

### 3.3 Evolution and evolvability of robustness

The evolution of robustness was studied through individual-based simulations, in which all individuals were characterized by their genotype (a 6-gene network) and a set of phenotypes (gene expressions and network robustness). Gene expressions for 3 out of 6 genes were under stabilizing selection. In addition to stabilizing selection on gene expression, robustness indicators were directly selected towards more or less sensitivity. This settings allows for a slight, indirect selection pressure towards more robustness to mutations in all simulations, as a result of the selection for genetic canalization due to stabilizing selection. (lower scores for  $\rho_M$ , and for the correlated trait  $\rho_m$ , Figure 3, black circles).

Direct selection on all robustness components lead to a response, showing that robustness is evolvable. Yet, the evolutionary potential of the robustness indicators

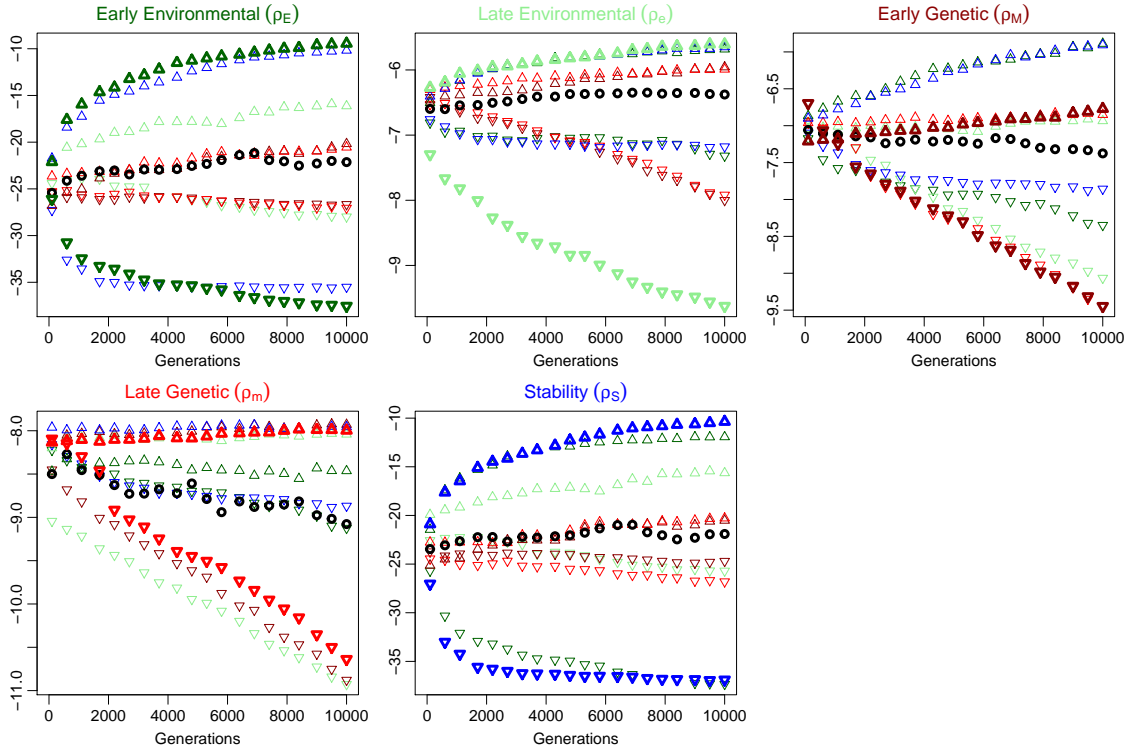


Figure 3: The evolution of all five robustness indicators (five figure panels) was recorded for 10,000 generations in individual-based simulations. The figures show the average robustness over 20 replicated simulations. The control simulations (black circles) correspond to stabilizing selection only. Colored symbols correspond to simulations in which various robustness indicators were selected up or down (upward or downward triangles). Bold-faced symbols indicate the result of direct selection (the robustness indicator displayed in the panel was directly selected), while thin symbols stand for indirect selection (the response is the result of selection on another indicator, which can be identified based on its color).

differed substantially, as indicated by the differences in the Y-scales. Robustness indicators being all homogeneous to a variance of gene expression, they could be compared directly. The most evolvable robustness components are Stability ( $\rho_S$ ) and early environmental disturbances ( $\rho_E$ ), which can differ by up to 25 log units (11 orders of magnitude). In contrast, robustness to late environmental noise  $\rho_e$  and genetic changes ( $\rho_M$  and  $\rho_m$ ) only differed by 3 to 4 log units (i.e. a factor 10 to 100) after 10,000 generations of selection, although the selection response was still ongoing.

Selection on all robustness components also lead to an indirect response of all other components, which confirms a general genetic correlation. Direct selection on environmental canalization or gene expression stability can thus induce the evolution of genetic canalization, and *vice versa*. Indirect responses were generally smaller or similar to direct responses, except when selecting for more sensitivity for early mutations  $\rho_M$ . This could be a consequence from the canalizing selection on gene expression, which opposes the direct selection towards decanitized networks.

Differences in evolvability can be attributed to differences in the strength of genetic constraints, i.e. the propensity to disconnect robustness components. Simulations were run to test the long-term effect of antagonistic selection on all

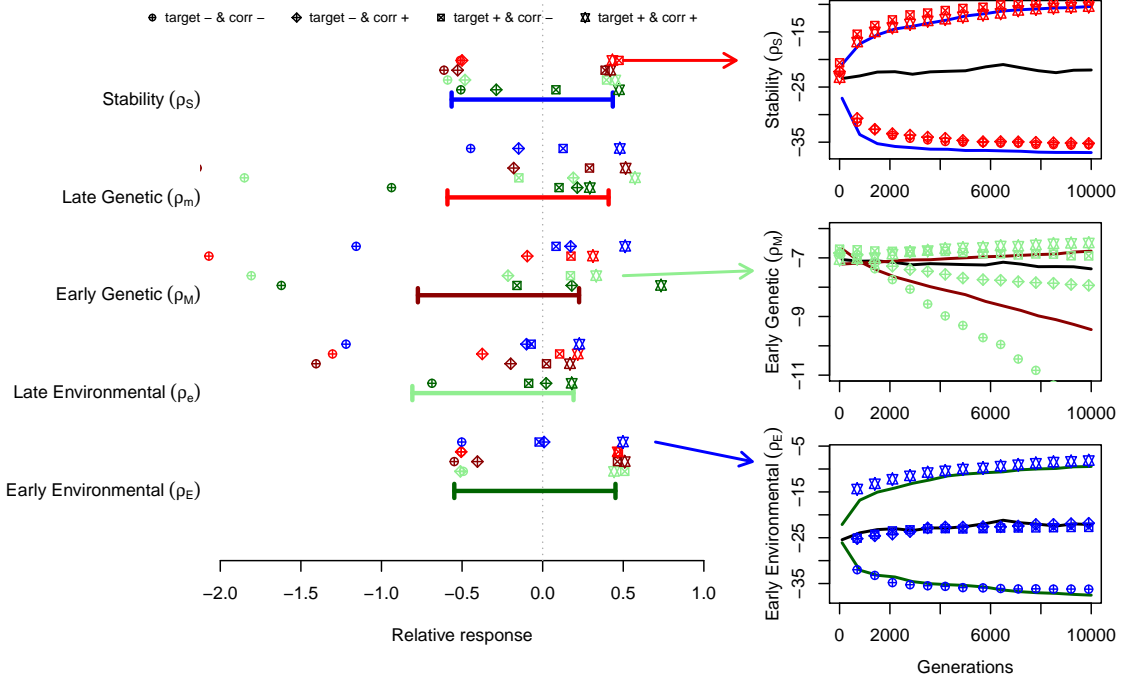


Figure 4: Bivariate response to selection (average over 20 simulation replicates) for all combinations of robustness indicators. Left: relative response (normalized by the up - down difference at generation 10,000) to univariate selection (thick horizontal lines) and bivariate selection (symbols). Zero stands for the control at generation 10,000. Four bivariate selection treatments were simulated: negative selection of both traits, negative for the target trait and positive for the correlated trait, positive for the target trait and negative for the correlated trait, and positive selection on both traits. Symbol colors stand for the correlated trait. Right panels: three characteristic dynamics representing different outcome for bivariate response (top: the target trait responded freely to selection in spite of antagonistic selection on the correlated trait; middle: the target traits responded, but at a lower pace as when selected alone; bottom: the target trait failed to respond to selection when the correlated trait was selected in the opposite direction.

pairs of robustness indicators (Fig. 4). Possible outcome included free evolution (the response to antagonistic selection was identical to selection on the target trait only), constrained evolution (the target trait responded slowly), or no evolution (the constraint was absolute and no response to antagonistic selection was observed). Each outcome was possible in practice (Fig. 4), but selection was able to trigger a partial or full response in the direction orthogonal to the main correlation in most cases. Most robustness components thus appeared to be at least partially evolvable independently from each other.

## 4 Discussion

Whether or not various robustness components of genetic architectures are independent is a key issue to understand why organisms are robust or sensitive to genetic or environmental disturbances. In particular, independent genetic bases of robustness components would call for independent evolutionary histories, while a pleiotropic genetic architecture could explain the evolution of nonadaptive

---

robustness components as a result of indirect selection. The analysis of the genetic correlations between five robustness components, based on a simple gene network model, results in a balanced answer: robustness components appear to be generally correlated, but the pleiotropy is not an absolute constraint, and most pairs of robustness components could be selected in divergent directions. Such a quantitative answer to the so-called 'congruence' hypothesis (Visser et al., 2003) would explain both how unselected robustness components could be partly driven by indirect selection and why various robustness-related features seem to have their own evolutionary history.

#### 4.1 Model

Gene regulation networks are popular candidates when attempting to model complex biological processes: they are at least partly built on solid and realistic principles (transcription factors can enhance or repress the expression of other genes), gene regulation plays a crucial role in most biological, physiological, and developmental mechanisms, and even modest-sized regulation networks display a wide diversity of possible outcomes, including homeostasis (stable equilibrium of gene expressions) (Stern, 1999), cyclic dynamics (Leloup and Goldbeter, 2003; Akman et al., 2010), or amplification of a weak signal (Hornung and Barkai, 2008). Conveniently, the phenotypic level considered as the output of a gene network (the expression level of all network genes) can be assimilated to a partial transcriptome, which opens the possibility for confrontation with empirical data.

The framework proposed by Wagner (1994) and Wagner (1996) is particularly popular in evolutionary biology to model gene network evolution due to its computational simplicity and efficiency, combined with a direct biological interpretation (each line of the regulation matrix is the set of transcription factor fixation sites in the promoter of a gene). In practice, multiple variants based on this original model have been derived, either to address specific questions, or to correct for unrealistic features. Here, I used a quantitative version of the model, in which gene expressions are scaled between 0 (no expression) and 1 (maximum expression), which was first proposed in Wagner (1994), although later work have often preferred binary networks (in which genes can be on/off, e.g. Wagner, 1996; Ciliberti et al., 2007), and a gene expression scaling between -1 and 1. Unlike in Wagner (1996) and Siegal and Bergman (2002), mutational effects were correlated in my simulations (the value of the mutant allele was drawn in a Gaussian centered around the value of the parental allele), which allows for cumulative evolution. Finally, the sigmoid response function was made asymmetrical by introducing a constitutive expression parameter (as in e.g. Rünneburger and Le Rouzic, 2016) in order to avoid the unrealistically high expression of unregulated genes (half the maximum expression) from the default Wagner model.

Discrete time and simple matrix algebra were necessary to run evolutionary individual-based computer simulations, in which the network output needs to be calculated for thousands of individuals and thousands of generations. Using more realistic models based on continuous time and differential equations, non-linear regulation effects, and independent degradation and transcription rates would make the simulations impractical, with little benefit in terms of explanatory power. Computational constraints also limit the network size to a few dozen genes max, which is not enough to generate realistic levels of sparsity – simulated gene networks were too dense to be realistic. The simulated phenotypic target (maintaining a constant set of gene expressions) were also extremely simple compared to what gene networks are theoretically able to do (e.g. converging to different equilibria in different cell types, or controlling a complex dynamic of gene expression during the

---

development). However, the general conclusions from this study are (at least qualitatively) robust to most simulation parameters (Appendix 7), suggesting that they reflect general properties of the underlying genetic architecture.

## 4.2 Robustness indicators

There are potentially many ways to measure the robustness of a phenotypic trait. Here, five indicators were measured, in order to catch various (and potentially independent) aspects of what is generally defined as robustness. The sensitivity to inherited mutations ( $\rho_M$ ) is probably the most popular one, as it is central to the discussion around the evolution of canalization (Waddington, 1959; Wagner, 1996; Fares, 2015). The sensitivity to environmental perturbations is also unavoidable, although its implementation in a gene network model is less straightforward. Here, it was calculated as both the sensitivity of the network to disturbance in the initial expression state ( $\rho_E$ ), which measures the size of the basin of attraction of the optimal expression pattern, and as the strength of the stability of the equilibrium when disturbed ( $\rho_e$ ). These two measurements could be interpreted as developmental robustness and physiological homeostasis, respectively, as they quantify the response of the network to disturbances in the expression levels at different time scales. The robustness to mutations occurring after the network convergence ( $\rho_m$ ) was considered because it sets up an alternative to the genetic vs. environmental congruence hypothesis: in long-lived organisms, non-heritable (somatic) mutations participate to the ageing process (Kennedy et al., 2012), and ageing could be under direct selection. Thus, the robustness to somatic mutations could also drive indirectly the evolution of genetic canalization. Finally, the gene network stability ( $\rho_S$ , amplitude of the fluctuations of gene expressions) was considered as a robustness component because it has been proven to drive an indirect response of genetic canalization, based on very similar model (Siegal and Bergman, 2002).

These indicators were chosen based on the possibility to measure them in numerical simulations. Although the empirical assessment of the correlation between robustness components would be way more convincing than a theoretical study, defining similar measurements from experimental datasets could be challenging. For instance,  $\rho_M$  and  $\rho_E$  could, at least in theory, be estimated as the variance in gene expression across genetic backgrounds or across environmental conditions, respectively. Measuring  $\rho_m$  environmentally could be more complicated, as it would likely be confounded with other ageing mechanisms. In contrast, the empirical distinction between e.g.  $\rho_e$  and  $\rho_S$  relies on discriminating internal vs. external sources of noise, and might be in practice impossible. In all cases, gene expression data are generally quite noisy and their analysis necessitate heavy corrections to prevent multiple testing issues. Studying empirically the robustness and evolvability of molecular and morphological traits has long been considered as a challenging task, but methodological and technological progress has recently brought new concrete perspectives (Payne and Wagner, 2019).

Some popular measurements of developmental robustness were not considered here for technical reasons. For instance, fluctuating asymmetry (the variance between the same phenotypic trait measured in the right and the left body parts of symmetric organisms) is a convenient measurement of microenvironmental effects on the development (Debat and David, 2001; Leamy and Klingenberg, 2005), but it has no equivalent at the level of gene expression in a regulation network. The deterministic sensitivity to a directional environmental gradient could also be used to measure phenotypic plasticity, which is central to the question of phenotypic robustness. Yet, there are several ways to model phenotypic plasticity in a gene

---

network (Masel, 2004; Odorico et al., 2018), and it requires a specific selection setup (different expression optima as a function of the environment). Because of this additional complexity, phenotypic plasticity was excluded from the focus of this work, although the evolution of plasticity of gene expression remains an intriguing and fundamental question. In particular, phenotypic plasticity (i.e. an adaptive lack of robustness to some environmental signal) may itself be canalized to genetic or other environmental disturbances (Stearns and Kawecki, 1994); considering reaction norms (a measurement of plasticity) as quantitative traits thus opens challenging questions about the adaptive evolution of the canalization of robustness traits.

## Conflict of interest disclosure

The author of this article declares that he has no financial conflict of interest with the content of this article.

## References

Akman, O. E., D. A. Rand, P. E. Brown, and A. J. Millar (2010). Robustness from flexibility in the fungal circadian clock. *BMC systems biology* 4.1, p. 88.

Azevedo, R. B., R. Lohaus, S. Srinivasan, K. K. Dang, and C. L. Burch (2006). Sexual reproduction selects for robustness and negative epistasis in artificial gene networks. *Nature* 440.7080, pp. 87–90.

Bergman, A. and M. L. Siegal (2003). Evolutionary capacitance as a general feature of complex gene networks. *Nature* 424.6948, pp. 549–552.

Carneiro, M. O., C. H. Taubes, and D. L. Hartl (2011). Model transcriptional networks with continuously varying expression levels. *BMC evolutionary biology* 11.1, p. 363.

Ciliberti, S., O. C. Martin, and A. Wagner (2007). Innovation and robustness in complex regulatory gene networks. *Proceedings of the National Academy of Sciences* 104.34, pp. 13591–13596.

Debat, V. and P. David (2001). Mapping phenotypes: canalization, plasticity and developmental stability. *Trends in Ecology & Evolution* 16.10, pp. 555–561.

Draghi, J. and G. P. Wagner (2009). The evolutionary dynamics of evolvability in a gene network model. *Journal of evolutionary biology* 22.3, pp. 599–611.

Eddelbuettel, D. and J. J. Balamuta (2017). Extending extitR with extitC++: A Brief Introduction to extitRcpp. *PeerJ Preprints* 5, e3188v1. ISSN: 2167-9843.

Eshel, I. and C. Matessi (1998). Canalization, genetic assimilation and preadaptation: a quantitative genetic model. *Genetics* 149.4, pp. 2119–2133.

Espinosa-Soto, C., O. C. Martin, and A. Wagner (2011). Phenotypic plasticity can facilitate adaptive evolution in gene regulatory circuits. *BMC Evolutionary Biology* 11.1, p. 5.

Espinoza-Soto, C., O. C. Martin, and A. Wagner (2011). Phenotypic robustness can increase phenotypic variability after nongenetic perturbations in gene regulatory circuits. *Journal of evolutionary biology* 24.6, pp. 1284–1297.

Fares, M. A. (2015). The origins of mutational robustness. *Trends in Genetics* 31.7, pp. 373–381.

Fierst, J. L. and P. C. Phillips (2015). Modeling the evolution of complex genetic systems: The gene network family tree. *Journal of Experimental Zoology Part B: Molecular and Developmental Evolution* 324.1, pp. 1–12.

Flatt, T. (2005). The evolutionary genetics of canalization. *The Quarterly review of biology* 80.3, pp. 287–316.

---

Guyeux, C., J.-F. Couchot, A. Le Rouzic, J. M. Bahi, and L. Marangio (2018). Theoretical study of the one self-regulating gene in the modified wagner model. *Mathematics* 6.4, p. 58.

Hallgrímsson, B., R. M. Green, D. C. Katz, J. L. Fish, F. P. Bernier, C. C. Roseman, N. M. Young, J. M. Cheverud, and R. S. Marcucio (2019). “The developmental-genetics of canalization”. *Seminars in Cell & Developmental Biology*. Vol. 88. Elsevier, pp. 67–79.

Hermissen, J., T. F. Hansen, and G. P. Wagner (2003). Epistasis in polygenic traits and the evolution of genetic architecture under stabilizing selection. *The American Naturalist* 161.5, pp. 708–734.

Hornung, G. and N. Barkai (2008). Noise propagation and signaling sensitivity in biological networks: a role for positive feedback. *PLoS Comput Biol* 4.1, e8.

Kauffman, S. (1969). Homeostasis and differentiation in random genetic control networks. *Nature* 224.5215, pp. 177–178.

Kavecki, T. J. (2000). The evolution of genetic canalization under fluctuating selection. *Evolution* 54.1, pp. 1–12.

Kennedy, S. R., L. A. Loeb, and A. J. Herr (2012). Somatic mutations in aging, cancer and neurodegeneration. *Mechanisms of ageing and development* 133.4, pp. 118–126.

Klingenberg, C. P. (2019). Phenotypic plasticity, developmental instability, and robustness: The concepts and how they are connected. *Frontiers in Ecology and Evolution* 7, p. 56.

Le Cunff, Y. and K. Pakdaman (2012). Phenotype-genotype relation in Wagner’s canalization model. *Journal of Theoretical Biology* 314, pp. 69–83.

Le Rouzic, A., J. M. Álvarez-Castro, and T. F. Hansen (2013). The evolution of canalization and evolvability in stable and fluctuating environments. *Evolutionary Biology* 40.3, pp. 317–340.

Leamy, L. J. and C. P. Klingenberg (2005). The genetics and evolution of fluctuating asymmetry. *Annu. Rev. Ecol. Evol. Syst.* 36, pp. 1–21.

Leloup, J.-C. and A. Goldbeter (2003). Toward a detailed computational model for the mammalian circadian clock. *Proceedings of the National Academy of Sciences* 100.12, pp. 7051–7056.

Loison, L. (2019). “Canalization and genetic assimilation: Reassessing the radicality of the Waddingtonian concept of inheritance of acquired characters”. *Seminars in cell & developmental biology*. Vol. 88. Elsevier, pp. 4–13.

Masel, J (2004). Genetic assimilation can occur in the absence of selection for the assimilating phenotype, suggesting a role for the canalization heuristic. *Journal of evolutionary biology* 17.5, pp. 1106–1110.

Masel, J. and M. L. Siegal (2009). Robustness: mechanisms and consequences. *Trends in genetics* 25.9, pp. 395–403.

Milocco, L. and I. Salazar-Ciudad (2020). Is evolution predictable? Quantitative genetics under complex genotype-phenotype maps. *Evolution* 74.2, pp. 230–244.

Nijhout, H. F. (2002). The nature of robustness in development. *Bioessays* 24.6, pp. 553–563.

Nijhout, H. F., J. A. Best, and M. C. Reed (2019). Systems biology of robustness and homeostatic mechanisms. *Wiley Interdisciplinary Reviews: Systems Biology and Medicine* 11.3, e1440.

Odorico, A., E. Rünneburger, and A. Le Rouzic (2018). Modelling the influence of parental effects on gene-network evolution. *Journal of evolutionary biology* 31.5, pp. 687–700.

Payne, J. L. and A. Wagner (2019). The causes of evolvability and their evolution. *Nature Reviews Genetics* 20.1, pp. 24–38.

---

Pinho, R., E. Borenstein, and M. W. Feldman (2012). Most networks in Wagner’s model are cycling. *PloS one* 7.4, e34285.

R Core Team (2020). *R: A Language and Environment for Statistical Computing*. R Foundation for Statistical Computing. Vienna, Austria.

Rajon, E. and J. Masel (2013). Compensatory evolution and the origins of innovations. *Genetics* 193.4, pp. 1209–1220.

Rünneburger, E. and A. Le Rouzic (2016). Why and how genetic canalization evolves in gene regulatory networks. *BMC evolutionary biology* 16.1, pp. 1–11.

Schmalhausen, I. I. (1949). Factors of evolution: the theory of stabilizing selection.

Siegal, M. L. and A. Bergman (2002). Waddington’s canalization revisited: developmental stability and evolution. *Proceedings of the National Academy of Sciences* 99.16, pp. 10528–10532.

Smolen, P., D. A. Baxter, and J. H. Byrne (2000). Modeling transcriptional control in gene networks—methods, recent results, and future directions. *Bulletin of mathematical biology* 62.2, pp. 247–292.

Stearns, S. C. (2002). Progress on canalization. *Proceedings of the National Academy of Sciences* 99.16, pp. 10229–10230.

Stearns, S. C. and T. J. Kawecki (1994). Fitness sensitivity and the canalization of life-history traits. *Evolution* 48.5, pp. 1438–1450.

Stern, M. D. (1999). Emergence of homeostasis and “noise imprinting” in an evolution model. *Proceedings of the National Academy of Sciences* 96.19, pp. 10746–10751.

Visser, J. A. G. de, J. Hermisson, G. P. Wagner, L. A. Meyers, H. Bagheri-Chaichian, J. L. Blanchard, L. Chao, J. M. Cheverud, S. F. Elena, W. Fontana, et al. (2003). Perspective: evolution and detection of genetic robustness. *Evolution* 57.9, pp. 1959–1972.

Waddington, C. H. (1942). Canalization of development and the inheritance of acquired characters. *Nature* 150.3811, pp. 563–565.

— (1959). Canalization of development and genetic assimilation of acquired characters. *Nature* 183.4676, pp. 1654–1655.

Wagner, A. (1994). Evolution of gene networks by gene duplications: a mathematical model and its implications on genome organization. *Proceedings of the National Academy of Sciences* 91.10, pp. 4387–4391.

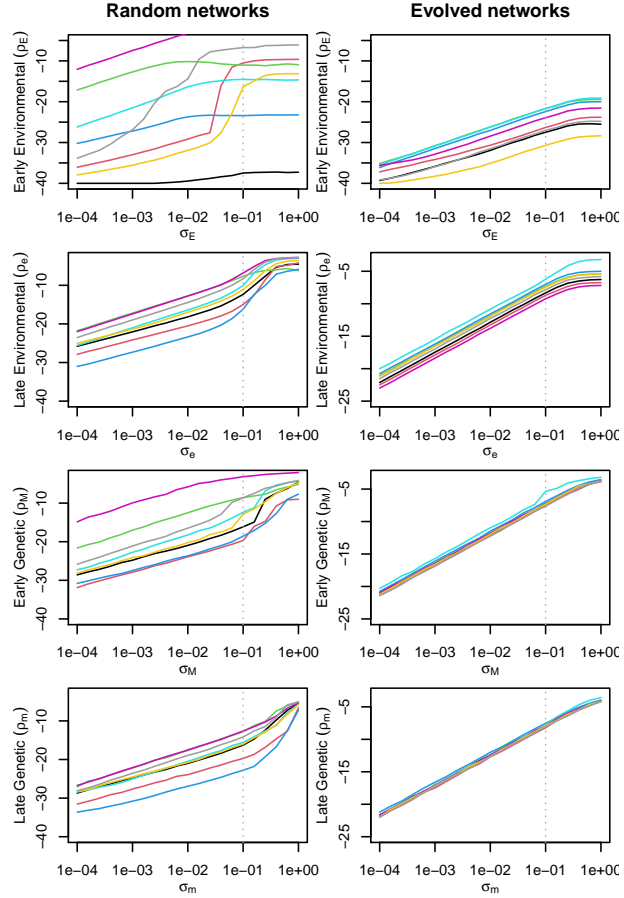
— (1996). Does evolutionary plasticity evolve? *Evolution* 50.3, pp. 1008–1023.

— (2013). *Robustness and evolvability in living systems*. Vol. 24. Princeton university press.

Wagner, G. P., G. Booth, and H. Bagheri-Chaichian (1997). A population genetic theory of canalization. *Evolution* 51.2, pp. 329–347.

## Appendix 1

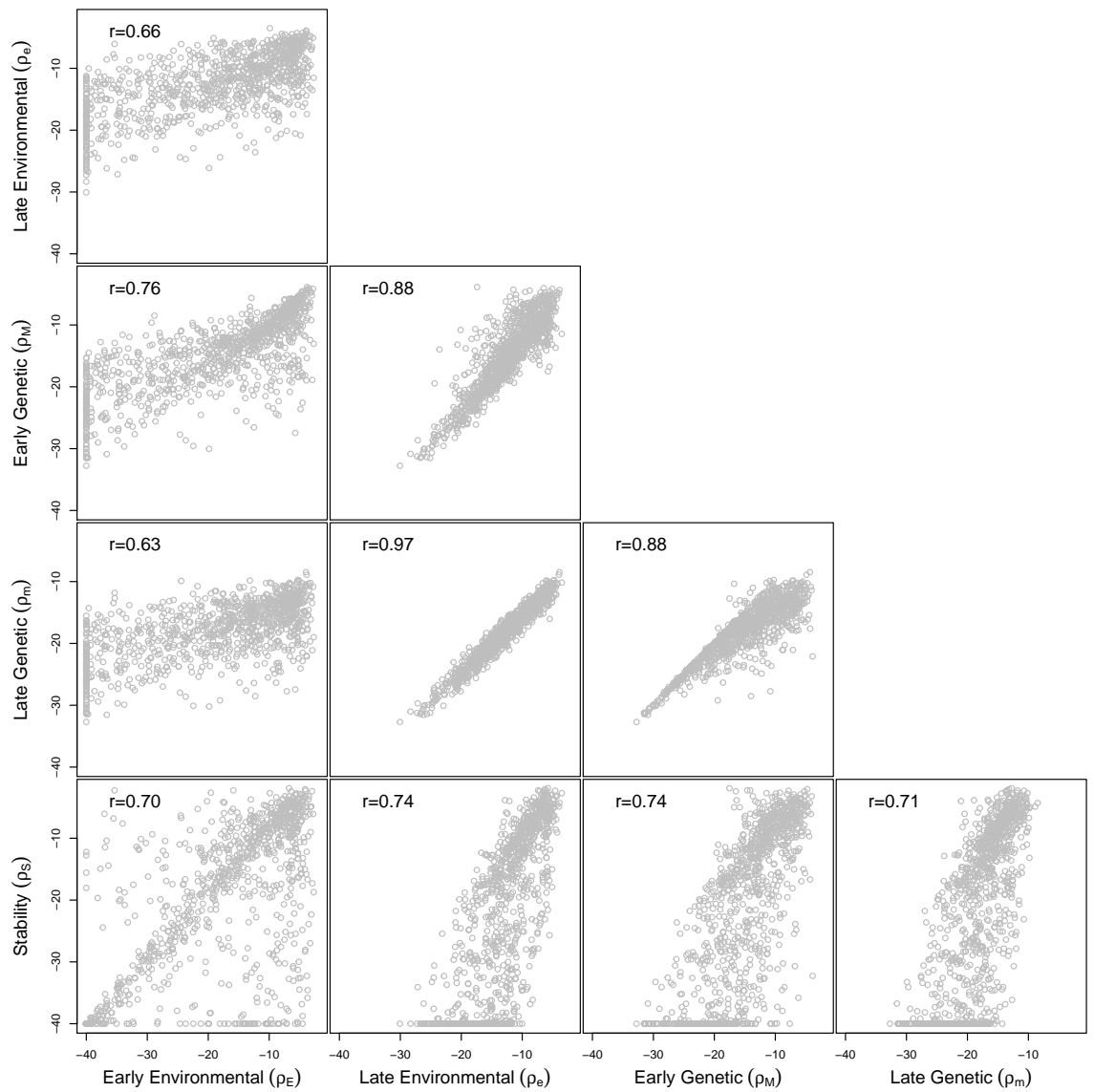
### Sensitivity of the robustness measurements to the magnitude of the disturbance



Four out of five robustness indicators ( $\rho_E, \rho_e, \rho_M, \rho_m$ ) depend on the magnitude of the disturbance. The figure displays the influence of the size of the disturbance on the robustness measurement (left: random networks, right: evolved networks). Robustness scores appear very reliable for evolved networks (the rank of different genotypes in terms of robustness does not depend on the size of the disturbance), while the picture is more messy for random networks, which can be differentially robust to large or small disturbances.

## Appendix 2

### Correlations among robustness indexes

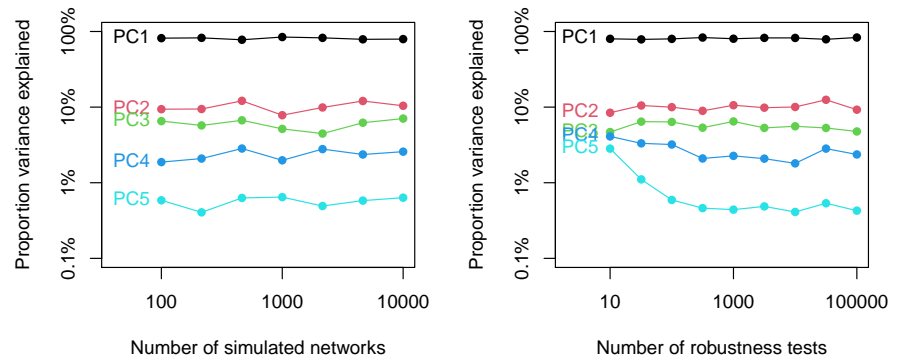


Correlations between all five robustness components among 10,000 random 6-gene networks ( $\mu_0 = 0, \sigma_0 = 1$ ).

---

## Appendix 3

### Sampling effects on Principal Components

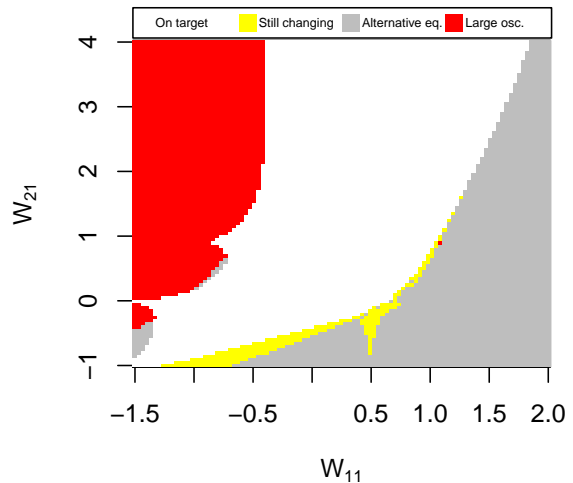


Influence of the sampling effect (number of networks and number of replicates  $R$  to estimate robustness) on the relative weight of the principal components. All PCs except the last one are robust to sampling.

---

## Appendix 4

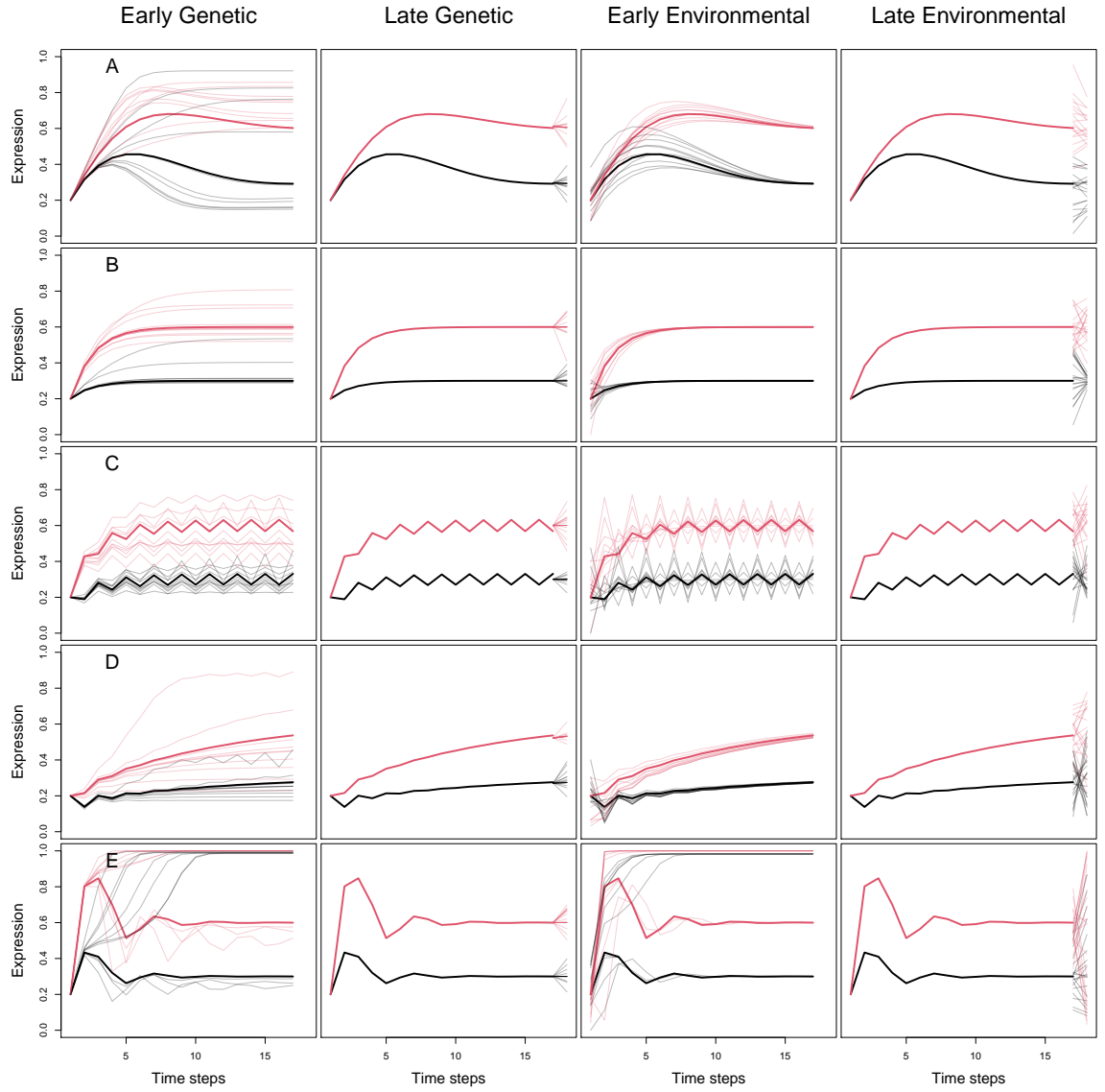
### Reasons for not reaching the desired equilibrium



Although equation 4 guarantees that an equilibrium exists at the target phenotypic expression, the equilibrium might not reachable in practice when simulating the gene network dynamics. The colored area in the figure corresponds to networks that failed to produce the target phenotype, each color representing a distinct reason; Yellow: network dynamics was slow and the final gene expression has not been reached yet after 16 time steps; Gray: an alternative equilibrium was reached (most of the time implying that one or both genes are either completely silenced to fully expressed). Red: The network steady state featured oscillations that were so large that they hit the maximum or minimum expression, shifting the average expression away from the target expression.

## Appendix 5

### Illustration of the robustness scores



The figure displays a subset of the replicated tests for four robustness indexes. Columns A to E correspond to the five networks described in Appendix 6. In each panel, the default (undisturbed) network kinetics is displayed as plain lines (black for gene 1, red for gene 2). By construction, all networks have an equilibrium at (0.3, 0.6). The network stability can be assessed from the amplitude of the cycles in the undisturbed kinetics. Network homeostasis (first line) was estimated by disturbing the expression state of the genes (for readability, the network response was expanded over several time steps). Environmental canalization (second line) was estimated by disturbing the initial state (semi-transparent lines). Genetic canalization (third line) was measured as the variance in the final state when mutating the network at the beginning of the development. Finally, the robustness to late mutations (last line) consisted in mutating the network after having reached the equilibrium.

---

## Appendix 6

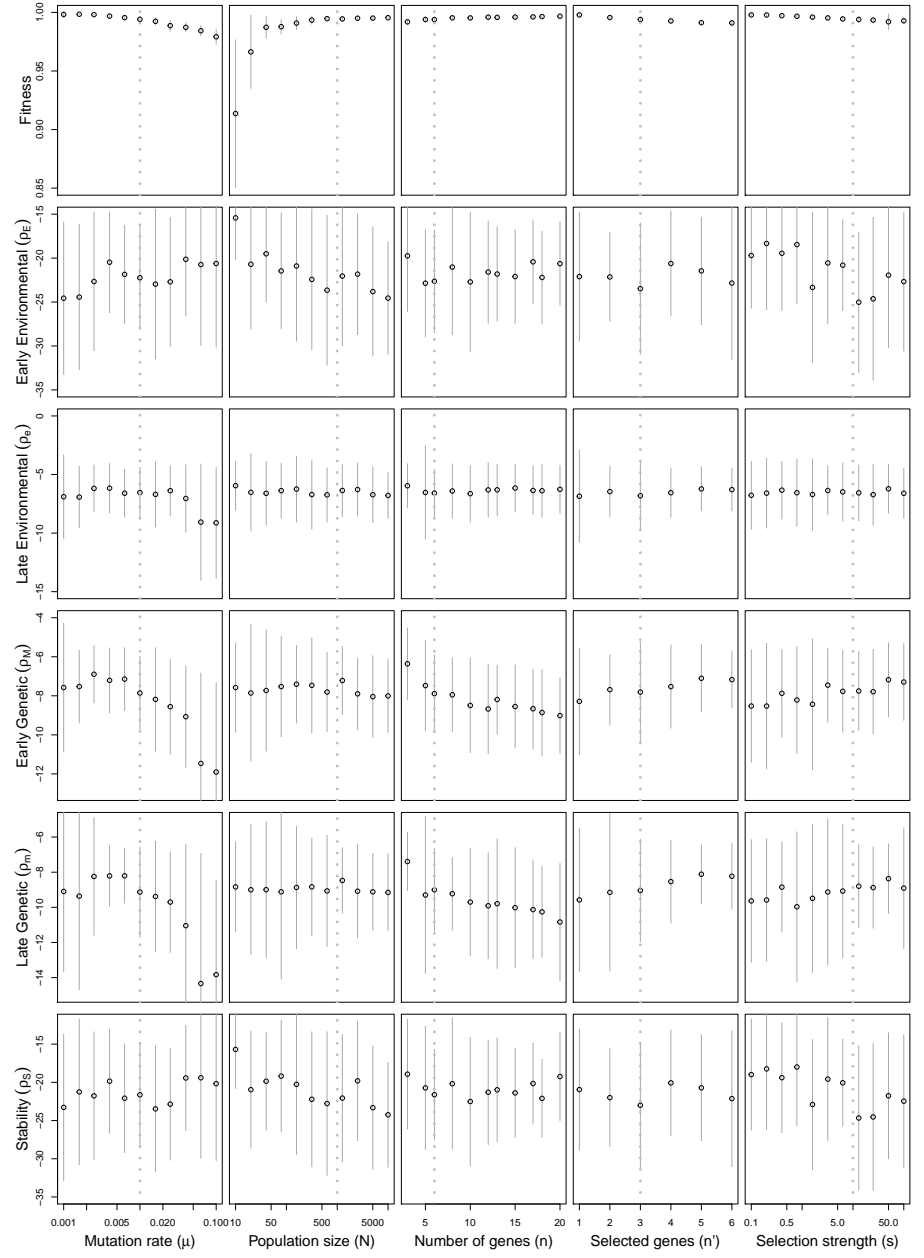
### Two-gene example networks

	$W_{11}$	$W_{21}$	$W_{12}$	$W_{22}$
A	0.70	0.20	-0.21	0.38
B	-0.30	0.30	0.29	0.33
C	-0.40	0.80	0.34	0.08
D	-1.00	-0.80	0.64	0.88
E	1.50	3.50	-0.61	-1.27

The five two-gene networks detailed in figures 2 and 5.

## Appendix 7

### Exploration of the parameter set



Influence of various simulation parameters (mutation rate  $\mu$ , population size  $N$ , total number of genes  $n$ , number of selected genes  $n'$ , and strength of selection  $s$ ) on fitness and robustness indexes at equilibrium. The figure reports the mean  $\pm$  standard deviation across 20 replicated simulations. Vertical dotted lines stand for the default parameter values in the simulations.